New Astronomy 98 (2023) 101938

Contents lists available at ScienceDirect

New Astronomy

journal homepage: www.elsevier.com/locate/newast

A Gaia based analysis of open cluster Berkeley 27

Devesh P. Sariya [a,*], Ing-Guey Jiang [a], D. Bisht [b,c], R.K. S. Yadav [d], G. Rangwal [b]

[a] Department of Physics and Institute of Astronomy, National Tsing-Hua University, Hsin-Chu, Taiwan
[b] Indian Institute of Astrophysics, Koramangala II Block, Bangalore, 560034, India
[c] Indian Center for Space Physics, 43 Chalantika, Garia Station Rd., Kolkata 700084, India
[d] Aryabhatta Research Institute of Observational Sciences, Manora Peak, Nainital 263002, India

ARTICLE INFO

Keywords:
Hertzsprung Russell diagram
Astrometry
Orbits
Open star clusters

ABSTRACT

In this paper, we have used the Gaia's Data Release-3 (DR3) data to study an intermediate-age open cluster Berkeley 27 (Be 27). A total of 131 most probable cluster members are picked within the cluster's radius based on the membership probability (>80%). The cluster's radius was estimated as 3.74 arcmin. The mean proper motion (PM) of Be 27 was determined to be $(\mu_\alpha cos\delta, \mu_\delta)$= $(-1.076 \pm 0.008, 0.152 \pm 0.007)$ mas yr^{-1}. The blue straggler stars (BSS) of the cluster were found to be located in the central region. Theoretical isochrones of metallicity Z_{metal} = 0.008 were compared to the color-magnitude diagram (CMD) of Be 27. As a result, a heliocentric distance of 4.8 ± 0.2 kpc and log (age) = 9.36 ± 0.03 were determined for Be 27. The Galactic orbits are derived using the Galactic potential model which demonstrate that Be 27 follows a circular path around the Galactic center. The cluster does not seem to be affected much by the tidal forces from the Galactic thin disk.

1. Introduction

Open clusters are the abundant star clusters in the Galactic disk region. The open clusters have a vast age range from a few million years to a few billion years. Due to their age range, the open clusters are used in studying the star formation process and stellar evolution (Lada and Lada, 2003; Kim et al., 2017). The component stars of an open cluster have similar age, heliocentric distance, metal content, etc. (Yadav et al., 2011). Stars of a cluster have a similar mean motion (Sariya et al., 2021a). Therefore, with the knowledge of the proper motion (PM) components of individual stars in the direction of a cluster, their membership status can be defined. Such a study provides a refined sample of cluster stars for the derivation of the basic parameters (Cudworth, 1997; Joshi et al., 2016; Bisht et al., 2020, 2021; Sariya et al., 2021a,b). Gaia satellite data has provided several essential results for our Galaxy and its constituents (e.g., Cantat-Gaudin et al., 2018; Soubiran et al., 2018; Gao, 2018; Castro-Ginard et al., 2019; Ding et al., 2021; Penoyre et al., 2022; Belokurov and Kravtsov, 2022). Be 27 ($\alpha_{2000} = 06^h51^m20.88^s$, $\delta_{2000} = +05°46'19.2''$; $l = 207°.781$, $b = 2°.609$ (Cantat-Gaudin et al., 2018)) is an intermediate-age open cluster. The cluster is located in the third Galactic quadrant towards the Galactic anti-center region. There exist a handful of previous studies of this cluster (Setteducati and Weaver, 1962; Hasegawa et al., 2004; Carraro and Costa, 2007; Donati et al., 2012). Hasegawa et al. (2004) have mentioned Be 27 as Biurakan 11 and found an age = 2 Gyr and Z_{metal} = 0.03 for this cluster. Carraro and Costa (2007) reported the cluster's age around 2 Gyr by fitting a solar metallicity isochrone. Donati et al. (2012) report an age between 1.5 to 1.7 Gyr for Be 27. As Donati et al. (2012) mentioned, Be 27 does not have a clear red giant branch and clump which causes some uncertainty in the parameters for this cluster. In such a scenario, it could be fruitful to fit a theoretical isochrone to a color-magnitude diagram (CMD) that has the field stars removed. We use the precise PMs from Gaia-DR3 to determine the membership status of the stars. The identification chart in 5 × 5 arcmin^2 area for Be 27 shown in Fig. 1 which is taken from the STScI Digitized Sky Survey.[1]

Details regarding the Gaia data used in this work are provided in Section 2. The field star decontamination, membership probability determination and analysis of the associated results are presented in Section 3. Using the most probable cluster members, some fundamental parameters of Be 27 are calculated in Section 4. In Section 5, we describe the orbital picture of the cluster. The conclusions of this work are presented in Section 6.

2. Data

We used the third data release from the Gaia satellite (Gaia Collaboration et al., 2016a,b, 2021). Gaia-DR3 contains the information about

* Corresponding author.
E-mail address: deveshpath@gmail.com (D.P. Sariya).
[1] https://archive.stsci.edu/cgi-bin/dss_form?

https://doi.org/10.1016/j.newast.2022.101938
Received 5 August 2022; Received in revised form 7 September 2022; Accepted 13 September 2022
Available online 17 September 2022

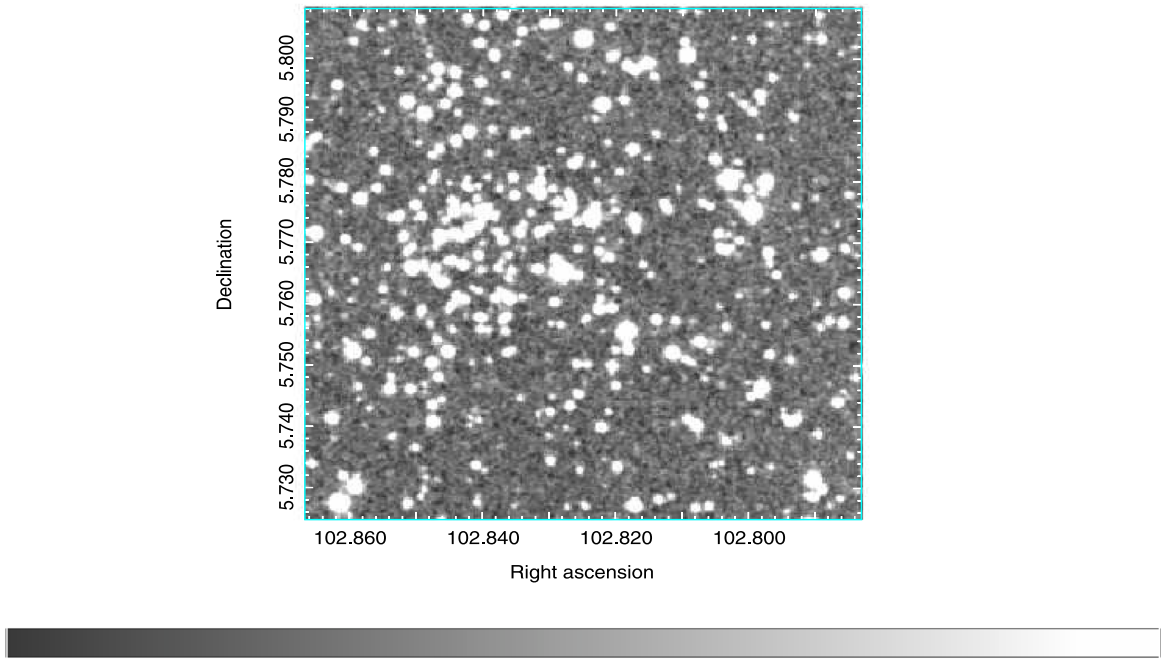

Fig. 1. Identification chart of Be 27 taken from the Digitized Sky Survey (DSS).

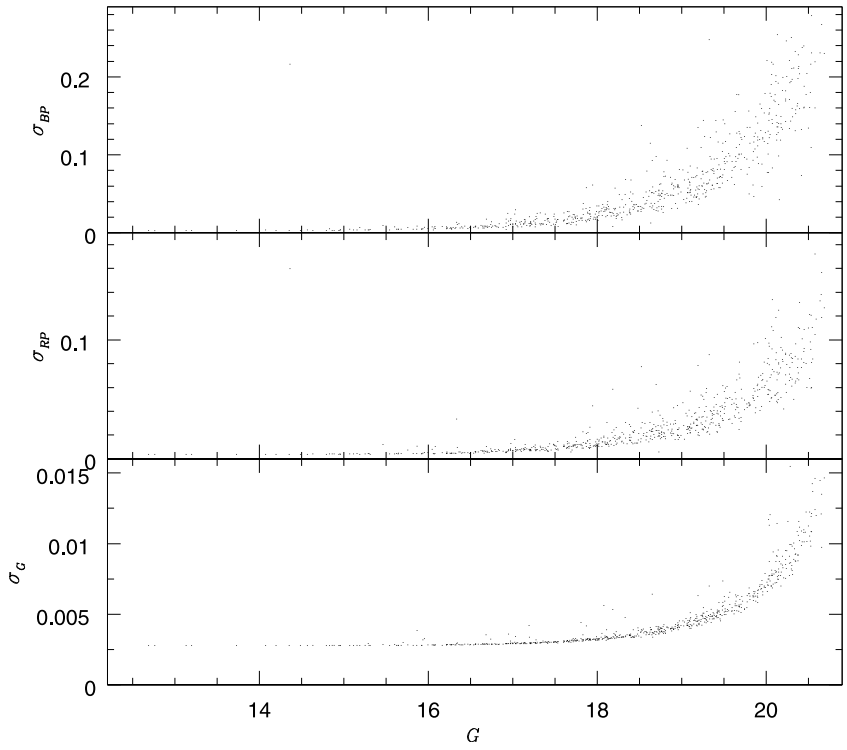

Fig. 2. Photometric errors in Gaia bands (G, BP and RP) with G magnitudes.

positions (α, δ), parallaxes and PMs $(\mu_\alpha \cos\delta, \mu_\delta)$. The data for radial velocities also exist in the Gaia-DR3. The photometry in Gaia data is available in three pass-bands: the white-light G, the blue BP, and the red RP bands. We show the photometric errors for these photometric bands with G mag in Fig. 2. In Fig. 3, we plot the errors in parallax and PMs with G mag. The value of the mean PM error for the studied stars is ~ 0.05 mas yr^{-1} for $G < 17$ mag. The error becomes ~ 0.2 mas yr^{-1} for stars with $G < 20$ mag. The mean error in parallax is ~ 0.28 mas for

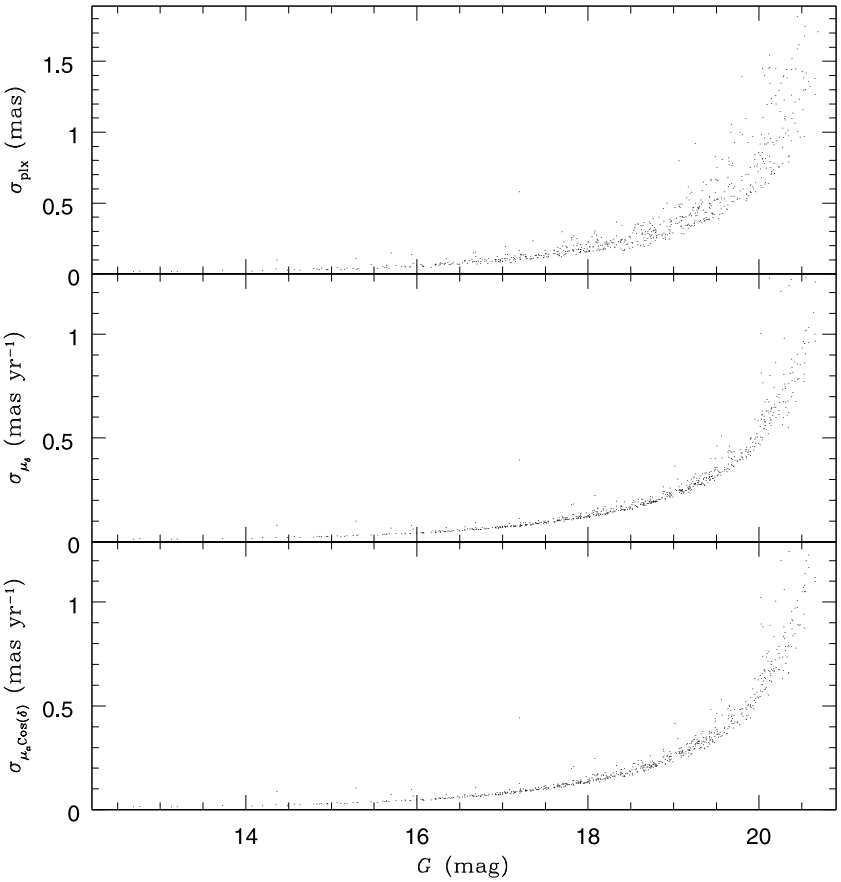

Fig. 3. The errors in parallax and PM components are plotted here against Gaia G magnitude.

stars brighter than 20 G mag. The median errors in G, BP and RP are ∼0.003, ∼0.03 and ∼0.02 for $G < 20$ mag.

3. Cluster membership

3.1. Vector point diagrams

The PMs can be used to distinguish cluster member stars from the field stars in the same direction as the cluster. For this purpose, we initially plot between both components of the PMs ($\mu_\alpha \cos\delta$, μ_δ). The resulting diagram is called the vector point diagram (VPD). Three separate VPDs for the stars in this work are shown in the top portions of Fig. 4. It is evident from the VPDs that the cluster's member stars tend to be located around a common point. The corresponding G versus $(BP - RP)$ CMDs of Be 27 are shown in the lower portion of the same figure. To make sure the inclusion of only the stars whose PMs are measured more precisely by Gaia, we put a cut-off limit of PM error < 1 mas yr^{-1} and parallax errors less than one mas.

The VPD has a circle of radius 0.3 mas yr^{-1} which indicates our preliminary cluster membership criterion. We also do not find a clear red giant branch and clump in the CMD constructed in the middle section of Fig. 4 as stated by Donati et al. (2012).

3.2. Membership probabilities

In Section 3.1, we presented a robust method to decontaminate field stars. However, we can do more analysis with the precise PMs from Gaia-DR3. This advantage of Gaia PMs led us to determine the membership probabilities for the stars lying in the observing direction of Be 27. We used the method presented by Balaguer-Núñez et al. (1998) to determined the membership probabilities. This method was previously used for open and globular clusters (Sariya et al., 2018, 2021a,b; Bisht et al., 2020, 2021, 2022). Sariya et al. (2018) give a detailed description of this method.

We put a PM error cut-off of 1 mas yr^{-1} and another condition that the parallax error should be better than 1 mas while calculating the distribution functions defined in this method. These distribution functions are noted by ϕ_c^v (cluster star distribution) and ϕ_f^v (field star distribution), For the cluster stars, we found $\mu_{xc} = -1.08$ mas yr^{-1}, $\mu_{yc} = 0.16$ mas yr^{-1} . The dispersion value in the PMs of the cluster population is estimated to be $(\sigma_c) = \sim 0.06$ mas yr^{-1}. For the field stars, we found: $(\mu_{xf}, \mu_{yf}) = (-0.35, -0.29)$ mas yr^{-1} and $(\sigma_{xf}, \sigma_{yf}) = (0.57, 0.72)$ mas yr^{-1}.

The resulting membership probabilities (P_μ) are plotted with Gaia's G magnitude in the left panel of Fig. 5. In the right panel of this figure, we show a histogram of membership probabilities. Using the distribution in histogram, we decided to use stars with $P_\mu > 80\%$ as the most probable cluster members for further analysis of Be 27. In the left panel of Fig. 5, a horizontal dashed line is used to show this cut-off value of 80%.

Conclusively, we obtained 131 stars with $P_\mu > 80\%$ and lying within the limiting radius (3.74 arcmin, Section 4.1) of Be 27. We show these stars in the left panel of Fig. 6. In the right panel of Fig. 6, we plot the CMD of the stars with $P_\mu > 80\%$ according to the membership catalogue given by Cantat-Gaudin et al. (2018). It is clear from these two CMDs that as compared to Cantat-Gaudin et al. (2018), we provide the most probable cluster members of Be 27 to a deeper magnitude (G ∼19.4 mag).

We used Gaussian function fitting to the histograms of PM components ($\mu_\alpha \cos\delta$ and μ_δ) which is shown in Fig. 7. Thus, we obtained the values of mean PM of Be 27 = $(-1.076 \pm 0.008, 0.152 \pm 0.007)$ mas yr^{-1}. These values are quite close to the values (−1.091, 0.147 mas yr^{-1}) determined by Cantat-Gaudin et al. (2018)

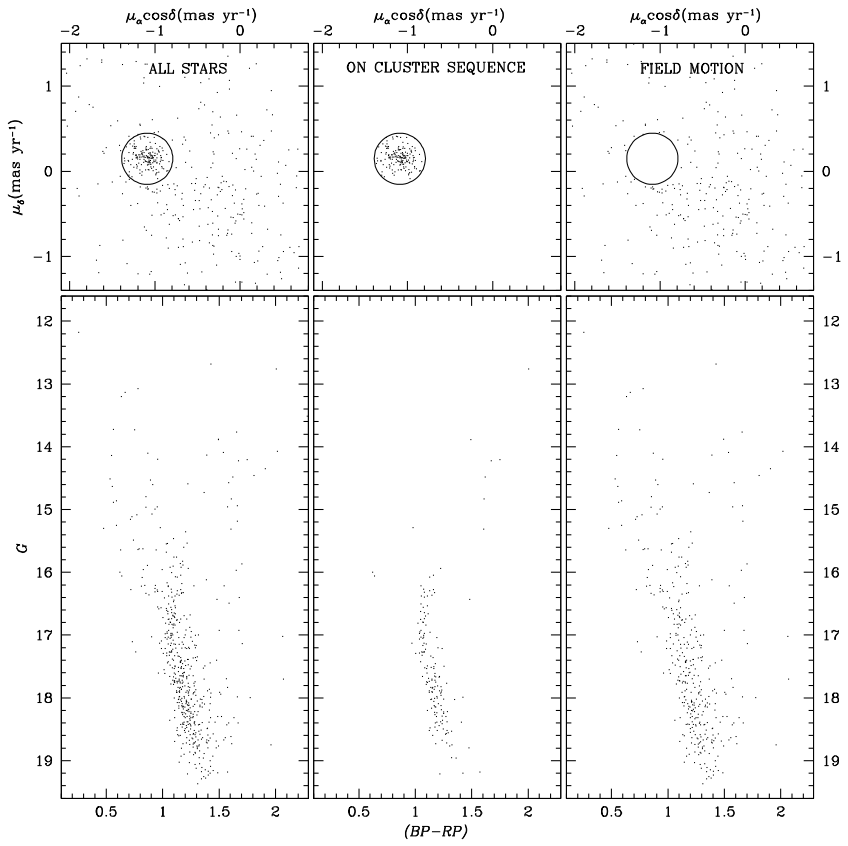

Fig. 4. (Top panels) The VPDs for the stars. (Bottom panels) The ($(BP-RP)$, G) CMDs. (Left) The entire sample of stars. (Center) The stars presumed as cluster members with their PMs lying within a radius of 0.3 mas yr^{-1} in the VPD. (Right) The decontaminated field stars.

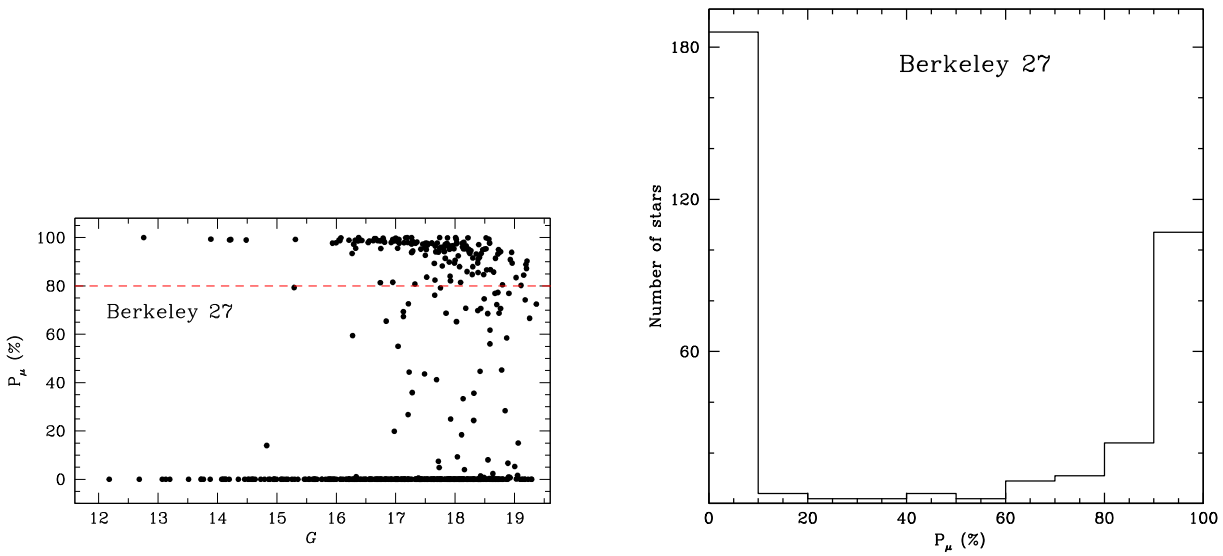

Fig. 5. (Left panel) Membership probability versus G magnitude. We also show here a horizontal dashed line for membership probability 80% above which we consider a star as the most probable cluster member. (Right panel) Histogram of membership probability of the stars in the field of Be 27.

The result for the parallaxes of Be 27 stars are shown in Fig. 8. The left panel of this figure presents histograms of all the stars in our study along with the histogram for the most probable cluster members. A Gaussian fit to the histogram for the most probable cluster member is shown in the right panel of Fig. 8. Our analysis gives us a value of 0.246 ± 0.011 mas for the mean parallax of Be 27.

3.2.1. *The BSS of Be 27*

The presence of BSS in a stellar system is a symbol of the 'delayed' evolution for certain stars. The origin of this population of BSS can be attributed to the mechanisms like mass transfer and merging due to collisions (Sandage, 1953; McCrea, 1964; Zinn and Searle, 1976; Hills and Day, 1976).

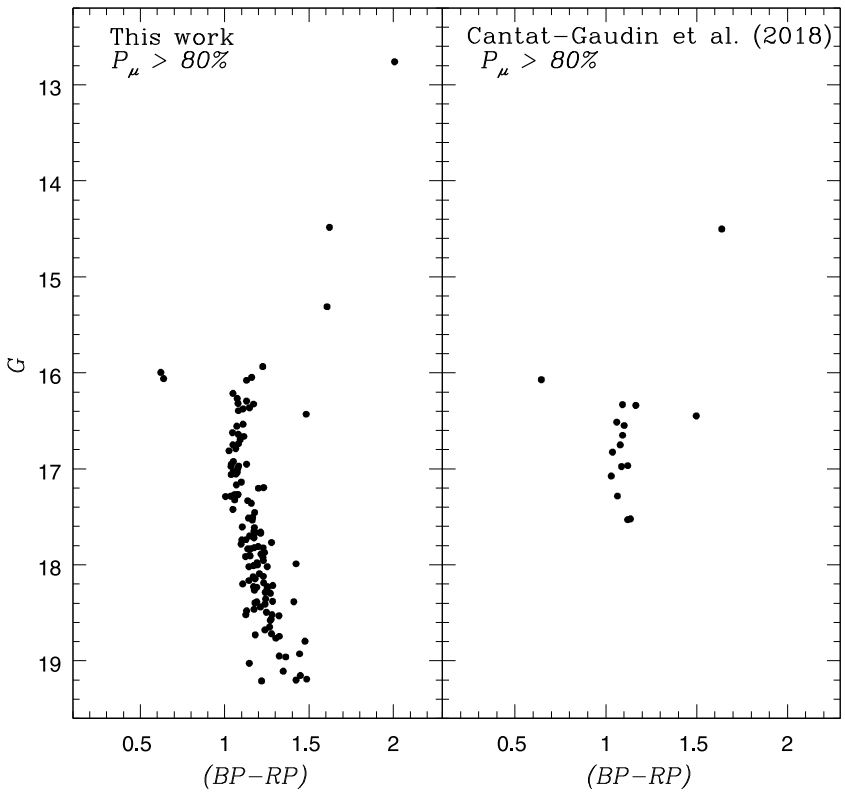

Fig. 6. Shown **here are the CMDs** of the most probable cluster members of Be 27 from our analysis (left panel) and from Cantat-Gaudin et al. (2018) (right panel).

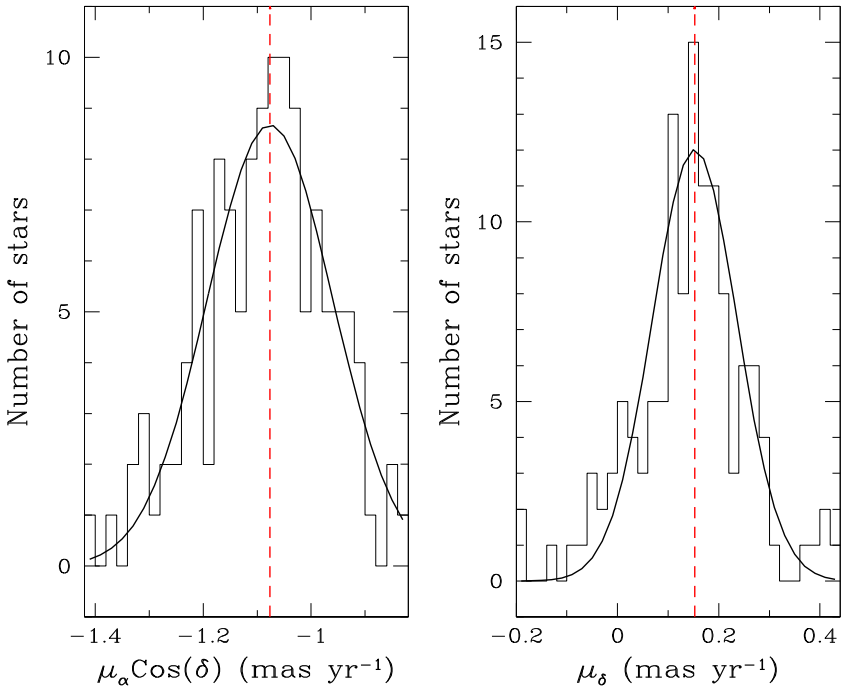

Fig. 7. Histograms for the components of PM with a Gaussian fitting done to determine the mean PM values. The resulting mean values are shown by the vertical dashed lines in both panels.

We detected two BSS as the most probable cluster members of Be 27. Their position in the CMD is shown in Fig. 9. Ferraro et al. (2012) defined three classes of BSS based on the radial distribution of the BSS (see Sariya et al., 2021b). The two BSS of Be 27 are located at a radial distance of 0.47 and 0.49 arcmin. Considering that both BSS are centrally located (within 0.5 arcmin), we can say that Be 27 belongs to

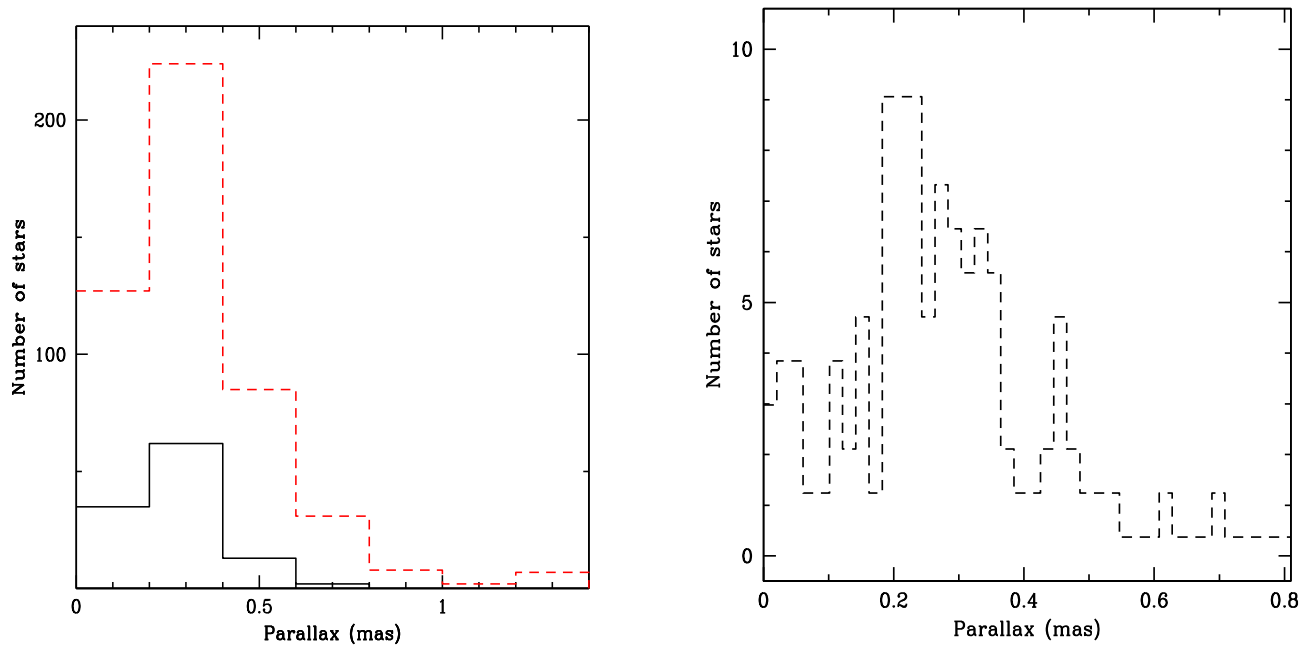

Fig. 8. (Left) Histogram of Gaia-DR3 parallaxes for all stars in shown by the red dashed line while the solid black histogram presents the most probable cluster members. (Right) For the most probable cluster members, a Gaussian fit to the histogram provides the mean parallax value.

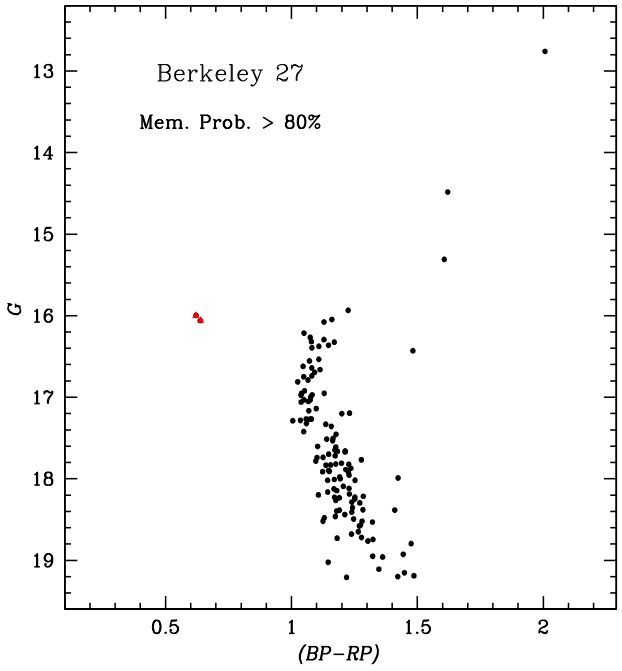

Fig. 9. The position of two BSS in the CMD of the most probable members of Be 27 is shown here by red triangles.

the family III of the BSS' radial distribution according to the criterion given by Ferraro et al. (2012). A higher density of the stars in the central region could be the reason behind this scenario.

4. Structural and fundamental parameters of Be 27

4.1. Radial density profile

A radial density profile (RDP) is constructed in order to determine the cluster's limiting radius. The cluster's data is first divided into several concentric rings. Then, for an ith zone, the stellar number density is calculated as: $R_i = \frac{N_i}{A_i}$, where N_i is the number of stars in that zone and A_i is the surface area of it. A King (1962) profile is fitted to the RDP.

The formula for the King profile is given below:

$$f(r) = f_{bg} + \frac{f_0}{1 + (r/r_c)^2} \quad (1)$$

where r_c, f_0, and f_{bg} are termed as core radius, central density, and the background density level. Fitting of the King profile to the RDP provides the structural parameters for the studied cluster. We calculated the following values of r_c, f_0 and f_{bg}: 0.56 ± 0.12 arcmin, 33.43 ± 9.36 stars per arcmin^2 and 0.10 ± 0.25 stars per arcmin^2.

The RDP along with the king profile is shown in Fig. 10. The background density along with the 3σ errors in it is also shown by the dashed lines in the figure.

In order to determine the limiting radius of Be 27, we used the following equation mentioned by Bukowiecki et al. (2011): $r_{lim} = r_c \sqrt{(\frac{f_0}{3\sigma_{bg}} - 1)}$. Thus, a limiting radius of 3.74′ was obtained for Be 27.

4.2. Age and distance

On the observed CMD of the most probable members of Be 27, we fitted theoretical isochrones provided by Bressan et al. (2012) to calculate the metallicity (Z_{metal}), age, heliocentric distance and reddening of Be 27. The isochrones' fitting to the CMD is shown in Fig. 11. These isochrones have a metallicity $Z_{metal} = 0.008$ and log(age) = 9.33, 9.36 and 9.39. Thus, the age of Be 27 is calculated to be 2.29 ± 0.15 Gyr. Also, the distance modulus ($m - M_G$) was derived as 14.26. Upon using the equations mentioned by Hendy (2018), we found the heliocentric distance of Be 27 = 4.8 ± 0.2 kpc. Donati et al. (2012) used several isochrones of different ages and metallicities. Among these, they also used Padova models with $Z_{metal} = 0.008$ which agrees with our results. Kharchenko et al. (2013) catalogue lists the log(age) and distance values of this cluster as 9.30 and 5.042 kpc. These literature values agree with our results within the given errors.

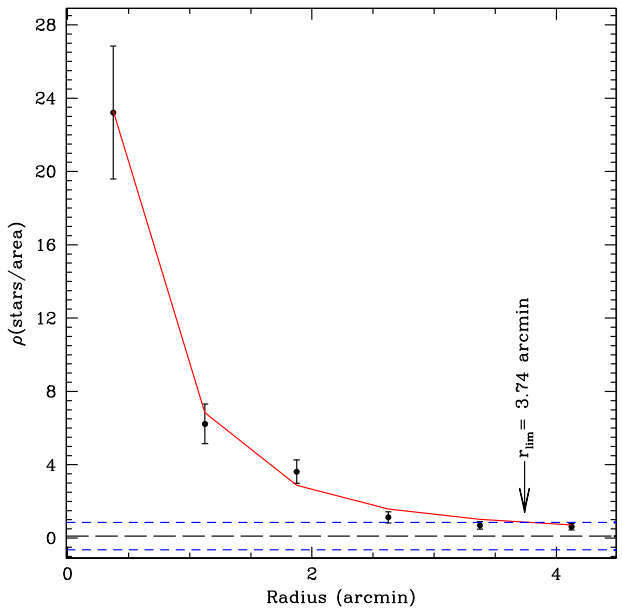

Fig. 10. The radial density profile for Be 27. The King (1962) profile is shown by a curve. The background density with 3σ errors is shown by the horizontal dashed lines.

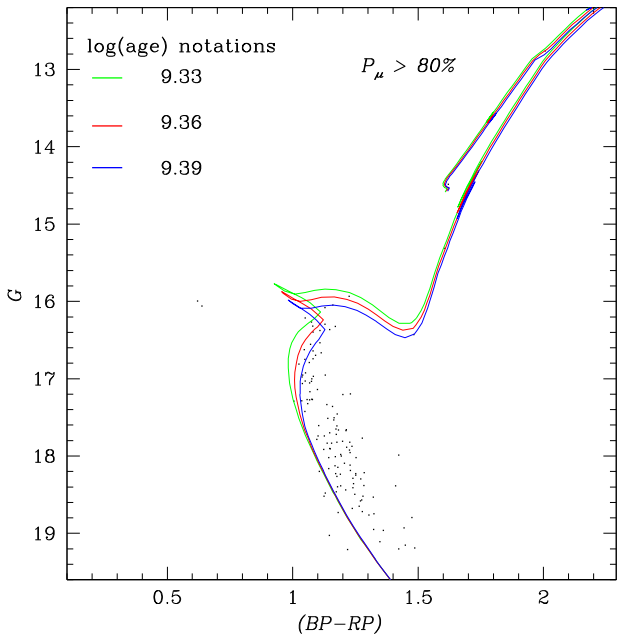

Fig. 11. The Gaia based CMD of the most probable cluster members is matched with the theoretical isochrones provided by Bressan et al. (2012). The fitted isochrones have a metallicity Z_{metal} = 0.008 and log(age) = 9.33 ± 0.03.

5. The cluster's orbit in the Galaxy

Studying orbits is advantageous for understanding the stars, clusters, and Galaxies' formation and evolution processes. We utilized the method of Allen and Santillan (1991) to acquire the Galactic orbits of Be 27. Bajkova and Bobylev (2016) and Bobylev et al. (2017) have refined Galactic potential model parameters using the new observational data for the Galactocentric distance R ∼ 0 to 200 kpc. The equations considered for the utilized models are described by Rangwal et al. (2019). The main fundamental parameters, namely the cluster center (α, δ taken from Cantat-Gaudin et al. (2018)), mean PMs ($\mu_\alpha \cos\delta$, μ_δ), mean parallax, cluster's age and heliocentric distance ($d_\odot$) have been used to define the orbital parameters in Be 27.

We converted equatorial space and velocity components into Galactic-space velocity components. The Galactic center is considered at
($17^h45^m32^s.224$, $-28°56'10''$) and the North-Galactic pole is considered at ($12^h51^m26^s.282$, $27°7'42''.01$, (Reid and Brunthaler, 2004)). To apply a correction for Standard Solar Motion and Motion of the Local Standard of Rest (LSR), we employed the position coordinates of the Sun as (8.3, 0, 0.02) kpc and its velocity components as (11.1, 12.24, 7.25) km s^{-1} (Schonrich et al., 2010). The transformed parameters in Galactocentric coordinate system are listed in Table 1.

Fig. 12 shows the orbits of the cluster Be 27. The left panel of this figure indicates the cluster's motion in terms of distance from the Galactic center and Galactic plane, which shows a two dimensional (2D) side view of the orbits. In the middle panel, the cluster motion is described in terms of x and y components of Galactocentric distance, which shows a top view of orbits. The right panel of this figure indicates the cluster's motion in the Galactic disc with time. Be 27 follows a boxy pattern according to our analysis. The eccentricity value we obtained is close to zero. Hence, the studied cluster (Be 27) traces a circular path around the Galactic center. The birth and the present-day locations of Be 27 in the Galaxy are represented by the filled circles and the triangles as shown in Fig. 12. The various orbital parameters are thus obtained. These are listed in Table 2. Here, e denotes eccentricity, R_a is the apogalactic distance, R_p is perigalactic distance, Z_{max} is the maximum distance traveled by cluster from Galactic disc, E is the average energy of orbits, J_z is z component of angular momentum, T_R is the time period of the revolution around the Galactic center, and T_Z is the time period of vertical motion.

In these figures, we can see that the clusters' birth position as well as the present day position is in the thick disc of the Galaxy. Hence, the cluster should have had a minimal interaction with the Galactic thin disc. As a result, the cluster is not expected to be affected much by the Galactic tidal forces originating from thin disc. Also, Be 27 is not affected by the inner part of the Galaxy since it is orbiting outside the solar circle.

6. Conclusions

We presented a study of intermediate-age open cluster Be 27 using the Gaia-DR3 data. Gaia PMs were used to determine the most probable cluster members. The main conclusions of the current study are given below:

- The limiting radius of Be 27 is calculated as 3.74 arcmin using the RDP.
- We identified 131 most probable cluster members which are also lying within the limiting radius of the cluster. The mean PM of Be 27 is determined as ($\mu_\alpha \cos\delta$ and μ_δ) = (-1.076 ± 0.008, 0.152 ± 0.007) mas yr^{-1}.
- In the cluster's central area (within 0.5 arcmin) 2 most probable BSS are identified.
- Bressan et al. (2012) isochrones of metallicity Z_{metal} = 0.008 were fitted to the CMD of most probable cluster members. Thus, we determined the heliocentric distance of Be 27 = 4.8 ± 0.2 kpc. The cluster's log(age) is estimated to be 9.36 ± 0.03.
- The Galactic orbits and orbital parameters are evaluated for Be 27 using potential Galactic models. We found this cluster is orbiting in a boxy pattern outside the solar circle and traced the circular path around the center of the Galaxy.

Table 1
Position and velocity components in the Galactocentric coordinate system. Here R is the Galactocentric distance, Z is the vertical distance from the Galactic disc, U V W are the radial tangential and the vertical components of velocity respectively and ϕ is the position angle relative to the sun's direction.

Cluster	R (kpc)	Z (kpc)	U (km s^{-1})	V (km s^{-1})	W (km s^{-1})	ϕ (radian)
Be 27	12.7665	0.24	-35.35 ± 4.67	-236.19 ± 2.48	8.92 ± 1.53	0.18

Table 2
Orbital parameters obtained using the Galactic potential model.

Cluster	e	R_a (kpc)	R_p (kpc)	Z_{max} (kpc)	E (100 km s^{-1})^2	J_z (100 kpc km s^{-1})	T_R (Myr)	T_Z (Myr)
Be 27	0.0003	14.047	14.055	0.36	−8.59	−30.15	337.224	**135.265**

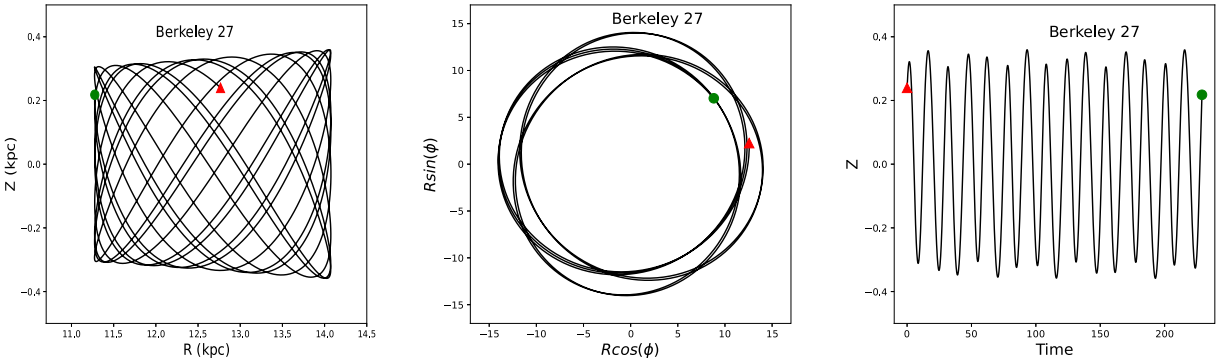

Fig. 12. Galactic orbits of the cluster Be 27 estimated with the Galactic potential model described in text in the time interval equal to the age of cluster. The left panel shows the side view and the middle panels show the top view of the orbits. The right panels shows the motion of the cluster in the Galactic disc with time. The filled circles and the triangles denote the birth and the present day positions of the cluster Be 27 in the Galaxy.

Declaration of competing interest

The authors declare that they have no known competing financial interests or personal relationships that could have appeared to influence the work reported in this paper.

Data availability

This paper has used publicly available Gaia DR3 data. The membership catalogue can be provided by the authors on request.

Acknowledgments

The authors are grateful to the reviewer for useful remarks on this paper. This work is supported by the grant from the Ministry of Science and Technology (MOST), Taiwan. The grant numbers are MOST 110-2112-M-007-035 and MOST 111-2112-M-007-035. This work has made use of data from the European Space Agency (ESA) mission Gaia (http://www.cosmos.esa.int/gaia), processed by the Gaia Data Processing and Analysis Consortium (DPAC, http://www.cosmos.esa.int/web/gaia/dpac/consortium). Funding for the DPAC has been provided by national institutions, in particular the institutions participating in the Gaia Multilateral Agreement.

References

Allen, C., Santillan, A., 1991. An improved model of the galactic mass distribution for orbit computations. Rev. Mexicana Astron. Astrofis 22, 255.
Bajkova, A.T., Bobylev, V.V., 2016. Rotation curve and mass distribution in the Galaxy from the velocities of objects at distances up to 200 kpc. Astron. Lett. 42, 567.
Balaguer-Núñez, L., Tian, K.P., Zhao, J.L., 1998. Determination of proper motions and membership of the open clusters NGC 1817 and NGC 1807. Astron. Astrophys. Suppl. Ser. 133, 387.
Belokurov, V., Kravtsov, A., 2022. From dawn till disc: Milky Way's turbulent youth revealed by the APOGEE+Gaia data. Mon. Not. R. Astron. Soc. 514, 689.
Bisht, D., Elsanhoury, W., Zhu, Q., et al., 2020. An investigation of poorly studied open cluster NGC 4337 using multicolor photometric and Gaia DR2 astrometric data. Astron. J. 160, 119.
Bisht, D., Zhu, Q., Yadav, R.K.S., et al., 2021. Multicolour photometry and gaia EDR3 astrometry of two couples of binary clusters (NGC 5617 and Trumpler 22) and (NGC 3293 and NGC 3324). Mon. Not. R. Astron. Soc. 503, 5929.
Bisht, D., Zhu, Q., Yadav, R.K.S., et al., 2022. A deep investigation of two poorly studied open clusters Haffner 22 and Melotte 71 in the Gaia era. Publ. Astron. Soc. Pac. 134, id.044201.
Bobylev, V.V., Bajkova, A.T., Gromov, A.O., 2017. Refinement of the parameters of three selected model galactic potentials based on the velocities of objects at distances up to 200 kpc. Astron. Lett. 43, 241.
Bressan, A., Marigo, P., Girardi, L., et al., 2012. PARSEC: Stellar tracks and isochrones with the PAdova and TRieste stellar evolution code. Mon. Not. R. Astron. Soc. 427, 127.
Bukowiecki, L., et al., 2011. Open clusters in 2MASS photometry, I. Structural and basic astrophysical parameters. Acta Astron. 61, 231.
Cantat-Gaudin, T., Jordi, C., Vallenari, A., et al., 2018. A Gaia DR2 view of the open cluster population in the Milky Way. Astron. Astrophys. 618, A93.
Carraro, G., Costa, E., 2007. Photometry of the five marginally studied open clusters collinder 74, Berkeley 27, Haffner 8, NGC 2509, and VdB-Hagen 4. Astron. Astrophys. 464, 573.
Castro-Ginard, A., Jordi, C., Luri, X., et al., 2019. Hunting for open clusters in Gaia DR2: The galactic anticentre. Astron. Astrophys. 627, A35.
Cudworth, K.M., 1997. Proper motion studies of star clusters and related objects. In: Proper Motions and Galactic Astronomy. ASP 127, San Francisco, CA, pp. 91–102.
Ding, X., Ji, K.-F., Li, X.-Z., et al., 2021. Fundamental parameters for 30 faint open clusters with Gaia EDR3 based on the more reliable members. Publ. Astron. Soc. Japan 73, 1486.
Donati, P., Bragaglia, A., Cignoni, M., et al., 2012. The anticentre old open clusters Berkeley 27, Berkeley 34 and Berkeley 36: New additions to the BOCCE project. Mon. Not. R. Astron. Soc. 424, 1132.
Ferraro, F.R., Lanzoni, B., Dalessandro, E., et al., 2012. Dynamical age differences among coeval star clusters as revealed by blue stragglers. Nature 492, 393.
Gaia Collaboration, Brown, A.G.A., et al., 2016a. Gaia data release 1. Summary of the astrometric, photometric, and survey properties. Astron. Astrophys. 595, A2.
Gaia Collaboration, Prusti, T., et al., 2016b. The Gaia mission. Astron. Astrophys. 595, A1.
Gaia Collaboration, Brown, A.G.A., et al., 2021. Gaia early data release 3. Summary of the contents and survey properties. Astron. Astrophys. 649, A1.
Gao, X., 2018. A machine-learning-based investigation of the open cluster M67. Astrophys. J. 869, 9.

Hasegawa, T., Malasan, H.L., Kawakita, H., et al., 2004. New photometric data of old open clusters in the anti-Galactic Center Region. Publ. Astron. Soc. Japan 56, 295.
Hendy, Y.H.M., 2018. Photometric and astrometric study of open cluster FSR 814 (Koposov 36) using SDSS/2MASS/PPMXL/Gaia DR2. NRIAG J. Astron. Geophys. 7, 180.
Hills, J.G., Day, C.A., 1976. Stellar collisions in globular clusters. Astrophys. Lett. 17, 87.
Joshi, Y.C., Dambis, A.K., Pandey, A.K., Joshi, S., 2016. Study of open clusters within 1.8 kpc and understanding the Galactic structure. Astron. Astrophys. 593, A116.
Kharchenko, N.V., Piskunov, A.E., Schilbach, E., 2013. Global survey of star clusters in the Milky Way, II. The catalogue of basic parameters. Astron. Astrophys. 558, A53.
Kim, S.C., Kyeong, J., Park, H.S., et al., 2017. BVI photometric study of the old open cluster Ruprecht 6. J. Korean Astron. Soc. 50, 79.
King, I., 1962. The structure of star clusters. I. An empirical density law. Astron. J. 67, 471.
Lada, C.J., Lada, E.A., 2003. Embedded clusters in molecular clouds. Annu. Rev. Astron. Astrophys. 41, 57.
McCrea, W.H., 1964. Extended main-sequence of some stellar clusters. Mon. Not. R. Astron. Soc. 128, 147.
Penoyre, Z., Belokurov, V., Evans, N.W., 2022. Astrometric identification of nearby binary stars - II. Astrometric binaries in the Gaia catalogue of nearby stars. Mon. Not. R. Astron. Soc. 513, 5270.
Rangwal, G., Yadav, R.K.S., Durgapal, A., Bisht, D., Nardiello, D., 2019. Astrometric and photometric study of NGC 6067, NGC 2506, and IC 4651 open clusters based on wide-field ground and Gaia DR2 data. Mon. Not. R. Astron. Soc. 490, 1383.
Reid, M.J., Brunthaler, A., 2004. The proper motion of Sagittarius A*. II. The mass of Sagittarius A*. Astrophys. J. 616, 872.
Sandage, A.R., 1953. The color-magnitude diagram for the globular cluster M 3. Astron. J. 58, 61.
Sariya, D.P., Jiang, I.-G., Bisht, D., et al., 2021a. A Gaia-based photometric and kinematic analysis of the old open cluster King 11. Astron. J. 162, 146.
Sariya, D.P., Jiang, I.-G., Sizova, M.D., et al., 2021b. Astrometric and photometric investigation of three old age open clusters in the Gaia era: Berkeley 32, Berkeley 98, and King 23. Astron. J. 161, 102.
Sariya, D.P., Jiang, I.-G., Yadav, R.K.S., 2018. A proper motion study of the globular cluster M12 (NGC 6218). Res. Astron. Astrophys. 18, 126.
Schonrich, Ralph, Binney, James, Dehnen, Walter, 2010. Local kinematics and the local standard of rest. Mon. Not. R. Astron. Soc. 403, 1829.
Setteducati, A.F., Weaver, M.F., 1962. Newly Found Stellar Clusters. Published by Radio Astr. Lab. University of California, Berkeley.
Soubiran, C., Cantat-Gaudin, T., Romero-Gómez, M., et al., 2018. Open cluster kinematics with Gaia DR2. Astron. Astrophys. 619, A155.
Yadav, R.K.S., Glushkhova, E.V., Sariya, D.P., et al., 2011. Optical photometric study of the open clusters Koposov 12, Koposov 53 and Koposov 77. Mon. Not. R. Astron. Soc. 414, 652.
Zinn, R., Searle, L., 1976. The masses of the anomalous cepheids in the Draco system. Agron. J. 209 (734).